



# On the effect of subgrade strength on the performance of geogrid-reinforced railway ballast

Romarc Desbrousses<sup>1\*</sup>, Mohamed Meguid<sup>1</sup>, and Sam Bhat<sup>2</sup>

<sup>1</sup>Department of Civil Engineering, McGill University, Montreal, QC, Canada

<sup>2</sup>Titan Environmental Containment Ltd., Iles des Chenes, MB, Canada

**Abstract.** This paper presents the results of a series of ballast box tests aimed at investigating the effectiveness of geogrid reinforcement in reducing track settlement in a 300mm-thick layer of railroad ballast supported by three different artificial subgrades. In each experiment, the ballast layer supports a model tie subjected to cyclic compressive loading applied at a frequency of 0.8Hz with stress extrema at the tie-ballast interface of 57kPa and 400kPa for a total of 40,000 cycles. The three artificial subgrades considered in this study have *CBR* readings of 25, 13, and 5. For each subgrade, four tests are performed whereby one corresponds to an unreinforced condition (i.e., no geogrid) and three are reinforced with a single geogrid placed at either 150mm, 200mm, and 250mm below the bottom of the tie. The results indicate that geogrids exhibit a superior ability to minimize the tie's settlement when the ballast layer is supported by a weak subgrade. The experiments further allude to the fact that the influence of the geogrid's placement depth is exacerbated by the subgrade's strength. In ballast layers supported by competent subgrades, the geogrid placement depth wields a marginal influence on the resulting tie settlement. However, the geogrid's location becomes a key factor in ballast beds underlain by soft subgrades, with geogrids placed closer to the bottom of the tie being the most effective at minimizing the tie settlement.

## 1 Introduction

Conventional railway tracks are constructed over a multi-layer ballasted substructure that comprises a ballast layer underlain by a subballast layer and a subgrade. Ensuring the satisfactory long-term performance of ballasted railway tracks relies, in part, on the response of the ballast layer and subgrade to the cyclic train loads the substructure must support during its service life [1, 2]. While the subgrade plays an important role in track stability and may contribute to the development of excessive track subsidence, the ballast layer is often recognized as one of the primary sources of track settlement owing to the unbound nature of its aggregate, its proximity to the ties, and its lack of appreciable lateral confinement [3, 4].

---

\* Corresponding author: [romarc.desbrousses@mail.mcgill.ca](mailto:romarc.desbrousses@mail.mcgill.ca)

When subjected to cyclic loading, ballast initially goes through a phase characterized by a rapid accumulation of non-recoverable deformations [5]. During this phase, its particles move down vertically and spread laterally in an attempt to reach a more stable and denser packing. The ballast layer's densification results in the generation of a tight interlock between neighboring ballast particles, thereby increasing the granular assembly's stiffness and reducing the rate at which settlement builds up [6]. The plastic settlement that occurs in the ballast layer leads to the downward and lateral displacement of the tracks, potentially jeopardizing the tracks' riding safety. This is generally remedied by performing expensive maintenance operations such as tamping to restore the track geometry to an acceptable level. However, the ballast aggregate degrades over time due to sustained exposure to train loading and repeated maintenance works in a process known as fouling characterized by the breakdown of the large ballast particles into finer ones [2, 5]. As ballast becomes fouled, it progressively loses its ability to perform its functions, paving the way for a renewed increase in the rate of settlement accumulation and further impacting the track alignment [7].

In response to these challenges, geogrids are increasingly being used to stabilize railroad ballast and minimize the accumulation of settlement in the granular layer [8–12]. Geogrids rely on their open structure, defined by large openings bordered by longitudinal and transverse ribs, to effectively reinforce unbound granular materials like ballast. The ballast particles surrounding a geogrid are able to strike through the geosynthetic's plane and become wedged in its apertures to develop a strong mechanical interlock. The geogrid then provides additional lateral confinement to the ballast aggregate, leading to a reduction in the material's lateral spreading, an increase in its stiffness, and an enhancement in the ballast's load-spreading ability which translates into smaller stresses being transferred to the underlying soil strata [13].

The ability of a geogrid to reinforce railroad ballast is strongly tied to the size of its apertures compared to that of the surrounding soil particles, its placement depth within the granular layer, and the compressibility of the underlying subgrade. Multiple studies have been devoted to investigating the relationship between the size of a geogrid's apertures ( $A$ ) and the mean diameter of the railroad ballast aggregate ( $D_{50}$ ) in which it is embedded. Results from direct shear tests and large-scale cyclic load tests suggest that optimum geogrid-ballast interlock is achieved for  $A/D_{50}$  ratios of 0.95-1.20 while acceptable interlock and poor interlocks are obtained with  $A/D_{50}$  ratios greater than 1.20 and smaller than 0.95 respectively [9, 12, 14, 15]. Additionally, large-scale cyclic loading experiments performed on geogrid-reinforced ballast such as those outlined in Table 1 have indicated that a geogrid is more effective at minimizing ballast vertical and lateral settlement when placed closer to the bottom of the ties although disturbance to the ballast layer caused by maintenance operations typically limits the lowest geogrid placement depth to 150mm below the ties. The benefit of embedding geogrid reinforcement in railroad ballast is also tied to the compressibility of the underlying subgrade, with geogrids being shown to be more effective at stabilizing ballast over weak subgrades [2, 5].

However, only a limited number of studies have sought to investigate how different subgrade strengths affect the performance of geogrids embedded in railroad ballast beds at different depths below the base of the ties. As such, the experimental campaign presented in this paper focuses on examining the effect of subgrade strength on the repeated load response of geogrid-reinforced railroad ballast. A total of thirteen large-scale ballast box tests are carried out on unreinforced and geogrid-reinforced ballast beds with geogrids located at different depths in the granular layer supported by different artificial subgrades of varying compressibility.

**Table 1.** Recommended geogrid placement depth for optimum ballast reinforcement.

Author(s)	Experiment(s)	Geogrid Depths	Optimum Depth	Observations
Bathurst et al. (1987)	Ballast Box Test	50mm, 100mm, 150mm, 200mm	200mm	-Maximum settlement reduction at placement depths of 50 and 100mm -50 and 100mm are not feasible in the field due to disturbance from maintenance works
Raymond (2002)	Cyclic Load Test & FEM	$D_r/B^*$ : 0.18 – 0.9	$D_r/B$ : 0.18 – 0.6	-Effect of reinforcement negligible when $D_r/B > 0.6$ -Benefit of geogrid becomes more pronounced with high number of loading cycles
McDowell & Stickley (2006)	Ballast Box Test	100mm, 200mm	200mm	-Better performance in terms of settlement with a geogrid depth of 200mm
Chen et al. (2012)	Ballast Box Test (DEM)	100mm, 150mm, 200mm, 250mm	200mm	-Geogrid is found to limit lateral ballast displacement within 50mm above and below its location
Indraratna et al. (2013)	Process Simulation Test	105mm, 170mm, 235mm, 300mm	235mm	-Geogrid most effective at limiting ballast vertical and lateral strains and ballast breakage at depth of 235mm
Sadeghi et al. (2023)	Ballast Box Test	100mm, 200mm	200mm	-Geogrid at 200mm results in smaller settlement, higher ballast stiffness, and lower ballast breakage

## 2 Methodology

The effect of subgrade strength on the cyclic loading behavior of geogrid-reinforced ballast is investigated by conducting a series of large-scale ballast box tests. The experiments are performed using a ballast box with plan dimensions of 915×1,290mm and a height of 600mm. The box's bottom surface consists of a steel plate supported by the laboratory's strong floor which may be covered by one of three rubber mats to simulate the presence of three different subgrades below the ballast specimens constructed in the box. The compressibility of each rubber pad is determined by conducting a California Bearing Ratio (*CBR*) test on each mat following the procedure outlined in ASTM D1883. The three rubber mats used in the tests give *CBRs* of 25, 13, and 5 while the box's bottom steel plate is considered to give a *CBR* of  $\infty$  (rigid).

Upon placing the relevant rubber mat at the bottom of the box, a 300mm-thick ballast layer is constructed in three 100mm-thick lifts. Each lift is compacted with a handheld vibrating plate compactor that applies a force of 30.1kgf over a 120×150mm area at a frequency of 133Hz. The ballast aggregate used in this study is crushed granite aggregate screened to conform with an AREMA No. 4 grading typical of the unbound aggregate used for mainline ballast. Upon placing the ballast layer in the box, a rectangular footing consisting of a steel I-beam with plan dimensions of 203×301mm is placed at the center of the granular layer's top surface.

When a geogrid-reinforced ballast bed is constructed, a 700×1,030mm sheet of geogrid is trimmed and placed at the desired placement depth. The geogrid used in the experiments is a large-aperture polypropylene biaxial geogrid with thick ribs and nodes designed to stabilize railroad ballast. The geogrid’s mechanical properties are summarized in Table 2.

**Table 2.** Properties of the large aperture biaxial geogrid [19, 20]

Aperture Size (mm)	Ribs/m	Rib Thickness (mm)	Tensile Strength (kN/m)		
			2% Strain	5% Strain	Ultimate
57/57	17	1.8/1.2	11/11	21/21	30/30

During each test, repeated compressive loading is applied to the ballast specimen at a frequency of 0.8Hz for a total of 40,000 repetitions by loading the steel footing using a pneumatic cyclic loading apparatus developed by the authors [5, 21] that comprises an 85kN pneumatic actuator, a 50kN load cell, a PID controller, an electronic pressure regulator, and a computer used for function generation purposes (see Figure 1). The compressive load applied to the model footing by the pneumatic actuator follows a sinusoidal waveform and gives rise to minimum and maximum compressive stresses of 57kPa and 400kPa respectively at the tie-ballast interface.

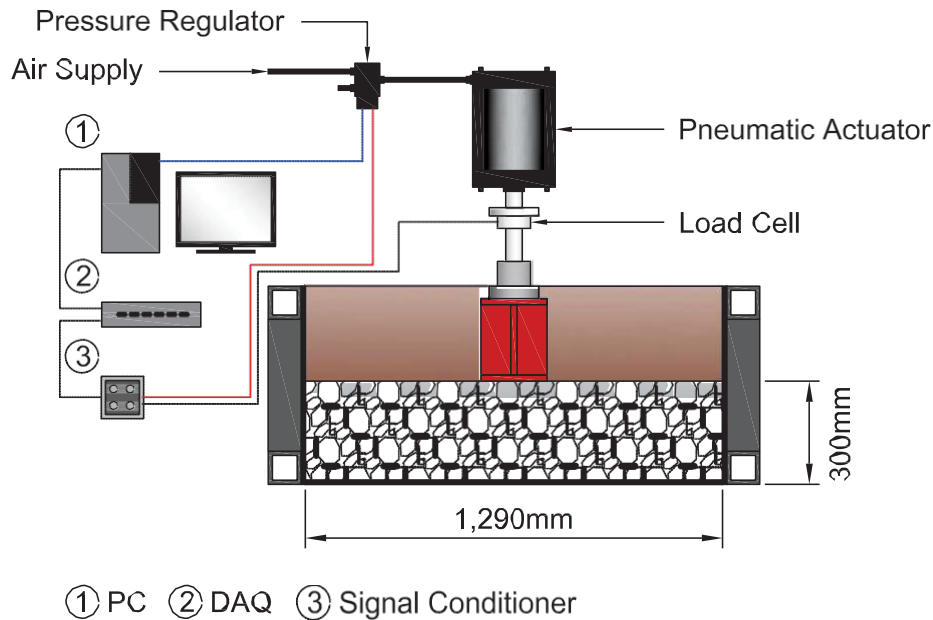


**Figure 1.** Pneumatic cyclic loading apparatus and ballast box.

The parameters monitored during a given test include the footing’s total displacement and the compressive load it is subjected to. The load is recorded by the 50kN load cell mounted on the pneumatic actuator’s piston rod while the footing’s settlement is monitored by four linear variable displacement transducers (LVDTs) placed at the four corners of the footing’s top surface. The sensors’ data is logged by a data acquisition system that samples data at a frequency of 100Hz.

Thirteen experiments are performed in the experimental campaign discussed herein. Four unreinforced tests are carried out on ballast beds supported by artificial subgrades having a *CBR* of ∞ (box’s rigid bottom steel plate), 25, 13, and 5 to establish benchmark results against which the performance of geogrid-reinforced ballast assemblies is compared. For each

artificial subgrade with *CBRs* of 25, 13, and 5, three experiments are carried out on ballast specimens reinforced with a single geogrid layer placed at a depth of 150mm, 200mm, and 250mm below the base of the footing.

### 3 Results

#### 3.1 Permanent settlement

The evolution of footing settlement over 40,000 load cycles, as recorded in unreinforced ballast box tests, is illustrated in Figure 2a. These tests were conducted with artificial subgrades having *CBRs* of  $\infty$  (rigid), 25, 13, and 5. In each case, the footing's subsidence initially experiences rapid buildup due to the densification of the unbound ballast particles under cyclic loading. As ballast densifies, its particles tightly wedge against each other, leading to the development of strong interlocking forces within the granular medium. This densification is accompanied by a reduction in the rate of settlement accumulation in the ballast layer. Figure 2a further highlights the crucial role of the subgrade in influencing the ballast's deformation response to cyclic loading. The smallest subsidence of 4.6mm occurs in the ballast layer supported by a rigid subgrade, followed by progressively larger settlements of 12.1mm, 24.5mm, and 35.0mm in ballast layers resting on subgrades with *CBRs* of 25, 13, and 5 respectively.

Figures 2b, 2c, and 2d depict the changes in the footing's vertical displacement recorded during unreinforced and reinforced ballast box tests conducted on artificial subgrades with *CBRs* of 25, 13, and 5 respectively. In experiments performed over a relatively stiff subgrade (*CBR* = 25), the inclusion of geogrids in the ballast bed leads to similar reductions in footing settlement, regardless of the reinforcement's placement depth. Ballast beds reinforced with a geogrid at a depth of 150mm, 200mm, and 250mm experience total settlements of 6.97mm, 6.13mm, and 7.33mm respectively compared to 12.1mm in the unreinforced condition.

However, the influence of the geogrid's placement depth becomes increasingly evident in tests conducted over softer subgrades. For a subgrade with a *CBR* of 13, the footing supported by a ballast layer reinforced with a geogrid placed 150mm below its base experiences a settlement of 10.4 compared with settlements of 11.3mm and 14.2mm when the geogrid is located at depths of 200mm and 250mm respectively. The impact of the geogrid's placement depth on the total footing settlement after 40,000 load cycles is further emphasized when dealing with an even weaker subgrade (*CBR* = 5). In this case, the footing supported by the ballast layer reinforced with a geogrid located 150mm below its base exhibits a total settlement of 12.82mm, compared with settlements of 15.74mm and 21.78mm for a geogrid placed at a depth of 200mm and 250mm respectively.

#### 3.2 Resilient settlement and damping ratio

To further analyze the response of geogrid-reinforced ballast under cyclic loading, the footing's resilient settlement, defined as the difference between its maximum and minimum settlement during a given load cycle, and the ballast's damping ratio, which provides a measure of the energy dissipated in the same load cycle, are computed. The final resilient settlement and damping ratio recorded at the end of each ballast box test are summarized in Table 3.

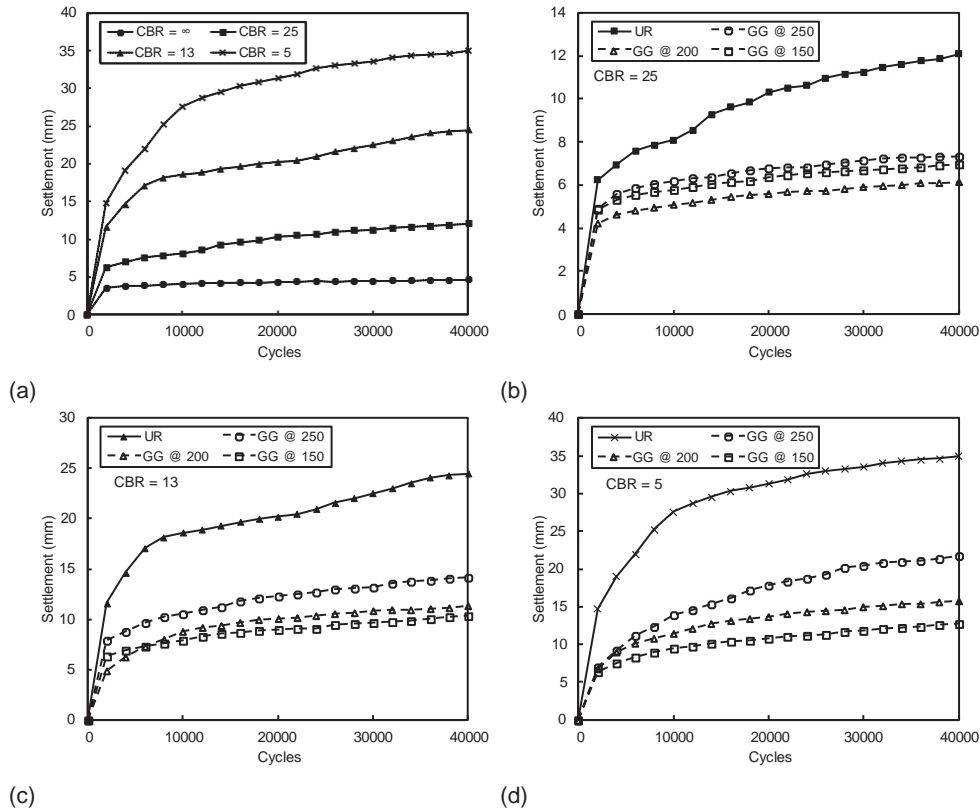


**Figure 2.** Footing settlement curves obtained in (a) unreinforced ballast layers and unreinforced and geogrid-reinforced ballast layers supported by a subgrade with a *CBR* of (b) 25, (c) 13, and (d) 5.

**Table 3.** Final resilient settlement and damping ratio recorded in each experiment.

Condition	<i>CBR</i> = 25				<i>CBR</i> = 13				<i>CBR</i> = 5			
	$\delta_r$ (mm)	<i>R</i> (%)	$D_r$	<i>R</i> (%)	$\delta_r$ (mm)	<i>R</i> (%)	$D_r$	<i>R</i> (%)	$\delta_r$ (mm)	<i>R</i> (%)	$D_r$	<i>R</i> (%)
UR	0.59	-	0.071	-	0.81	-	0.074	-	0.86	-	0.078	-
GG @ 150mm	0.53	9.4	0.063	11.2	0.65	19.5	0.072	1.9	0.74	14.0	0.075	4.2
GG @ 200mm	0.51	13.5	0.066	8.1	0.72	11.8	0.073	1.0	0.81	5.7	0.076	3.0
GG @ 250mm	0.50	14.9	0.062	13.7	0.70	13.6	0.074	-0.8	0.86	0.2	0.079	-1.3

$\delta_r$ : resilient settlement,  $D_r$ : damping ratio, *R*: reduction compared to UR, UR: unreinforced, GG: geogrid

The footing’s resilient settlement exhibits a similar sensitivity to the presence of geogrid reinforcement as its permanent displacement. In experiments conducted over a subgrade with a *CBR* of 25, similar reductions in elastic rebound of 9.4%, 13.5%, and 14.9% are obtained with geogrids located at depths of 150mm, 200mm, and 250mm respectively. However, the presence of weaker subgrades below the ballast bed magnifies the influence of the geogrid’s placement depth on the resilient settlement, with the geogrid located 150mm below the footing yielding the highest reduction in elastic rebound for subgrades with *CBR*s of 13 and 5 compared to the geogrids located at depths of 200mm and 250mm.

On the other hand, the damping ratio appears to be relatively insensitive to the presence of geogrid reinforcement. Although the inclusion of geogrids in ballast beds resting on a subgrade with a *CBR* of 25 decreases the damping ratio by approximately 10%, only negligible reductions in damping ratio are observed in the reinforced-ballast box tests performed on subgrades with *CBRs* of 13 and 5. This suggests that the ballast's damping ratio is primarily a function of the subgrade's strength.

## 4 Conclusion

The experimental campaign presented herein investigates the effect of subgrade strength on the performance of geogrid-reinforced ballast with a particular focus on the geogrid's placement depth. The key takeaway points from this study are as follows:

- x Geogrid-reinforced ballast layers supported by a competent subgrade (*CBR* of 25) are insensitive to the placement depth of geogrid reinforcement with similar reductions in permanent and resilient settlements being observed with geogrids located at depths of 150mm, 200mm, and 250mm,
- x For weaker subgrades (i.e., *CBRs* of 13 and 5), greater reductions in permanent and resilient settlement are achieved by placing geogrids at shallower depths,
- x Geogrids located 150mm below the footing are more effective than those located at depths of 200mm and 250mm at decreasing the footing's permanent and resilient settlement under cyclic loading in cases where the subgrade is weak, and
- x The damping ratio of geogrid-reinforced assemblies does not differ significantly from that of an unreinforced ballast assembly for a given subgrade, suggesting that the damping ratio is primarily a function of the subgrade strength.

## Acknowledgements

This research is funded by an NSERC Alliance grant in partnership with Titan Environmental Ltd. and by the McGill Engineering Vadasz Doctoral Fellowship. The authors are grateful for Dr. William Cook, Mr. John Bartczak, and Mr. Mike Stephens of the Jamieson Structures Laboratory at McGill University for their help in building the experimental setup used to perform the experimental campaign.

## References

1. Raymond, G.P.: Reinforced ballast behaviour subjected to repeated load. *Geotext. Geomembranes*. 20, 39–61 (2002). [https://doi.org/10.1016/S0266-1144\(01\)00024-3](https://doi.org/10.1016/S0266-1144(01)00024-3)
2. Desbrousses, R.L.E., Meguid, M.A.: Effect of subgrade compressibility on the reinforcing performance of railroad geogrids : insights from finite element analysis. In: *GeoCalgary 2022*. Canadian Geotechnical Society, Calgary, AB (2022)
3. Indraratna, B., Salim, W.: *Mechanics of Ballasted Rail Tracks: A Geotechnical Perspective*. Taylor & Francis Group (2005)
4. Lackenby, J., Indraratna, B., McDowell, G., Christie, D.: Effect of confining pressure on ballast degradation and deformation under cyclic triaxial loading. *Géotechnique*. 57, 527–536 (2007). <https://doi.org/10.1680/geot.2007.57.6.527>
5. Desbrousses, R.L.E., Meguid, M.A., Bhat, S.: Experimental Investigation of the Effects of Subgrade Strength and Geogrid Location on the Cyclic Response of Geogrid-Reinforced Ballast. *Int. J. Geosynth. Gr. Eng.* 9, 67 (2023). <https://doi.org/10.1007/s40891-023-00486-3>
6. Li, D., Hyslip, J., Sussmann, T., Chrismer, S.: *Railway Geotechnics*. CRC Press,

- London (2015)
7. Sussmann, T.R., Ruel, M., Chrismer, S.M.: Source of Ballast Fouling and Influence Considerations for Condition Assessment Criteria. *Transp. Res. Rec. J. Transp. Res. Board.* 2289, 87–94 (2012). <https://doi.org/10.3141/2289-12>
  8. Fischer, S.: Geogrid reinforcement of ballasted railway superstructure for stabilization of the railway track geometry – A case study. *Geotext. Geomembranes.* 50, 1036–1051 (2022). <https://doi.org/10.1016/j.geotexmem.2022.05.005>
  9. Indraratna, B., Hussaini, S.K.K., Vinod, J.S.: The lateral displacement response of geogrid-reinforced ballast under cyclic loading. *Geotext. Geomembranes.* 39, 20–29 (2013). <https://doi.org/10.1016/j.geotexmem.2013.07.007>
  10. Indraratna, B., Ngo, N.T., Rujikiatkamjorn, C.: Behavior of geogrid-reinforced ballast under various levels of fouling. *Geotext. Geomembranes.* 29, 313–322 (2011). <https://doi.org/10.1016/j.geotexmem.2011.01.015>
  11. Chen, C., McDowell, G.R., Thom, N.H.: Discrete element modelling of cyclic loads of geogrid-reinforced ballast under confined and unconfined conditions. *Geotext. Geomembranes.* 35, 76–86 (2012). <https://doi.org/10.1016/j.geotexmem.2012.07.004>
  12. Brown, S.F., Kwan, J., Thom, N.H.: Identifying the key parameters that influence geogrid reinforcement of railway ballast. *Geotext. Geomembranes.* 25, 326–335 (2007). <https://doi.org/10.1016/j.geotexmem.2007.06.003>
  13. Indraratna, B., Nimbalkar, S.: Stress-Strain Degradation Response of Railway Ballast Stabilized with Geosynthetics. *J. Geotech. Geoenvironmental Eng.* 139, 684–700 (2013). [https://doi.org/10.1061/\(ASCE\)GT.1943-5606.0000758](https://doi.org/10.1061/(ASCE)GT.1943-5606.0000758)
  14. Sadeghi, J., Tolou Kian, A.R., Ghiasinejad, H., Fallah Moqaddam, M., Motevalli, S.: Effectiveness of geogrid reinforcement in improvement of mechanical behavior of sand-contaminated ballast. *Geotext. Geomembranes.* 48, 768–779 (2020). <https://doi.org/10.1016/j.geotexmem.2020.05.007>
  15. Sadeghi, J., Tolou Kian, A.R., Khanmoradi, A., Chopani, M.: Behavior of sand-contaminated ballast reinforced with geogrid under cyclic loading. *Constr. Build. Mater.* 362, 129654 (2023). <https://doi.org/10.1016/j.conbuildmat.2022.129654>
  16. Bathurst, R.J., Raymond, G.P., Jarrett, P.M.: Performance of Geogrid-Reinforced Ballast Railroad Track Support. In: *Third International Conference on Geotextiles.* pp. 43–48. , Vienna, Austria (1986)
  17. Bathurst, R.J., Raymond, G.P.: Geogrid reinforcement of ballasted track. *Transp. Res. Rec.* 8–14 (1987)
  18. McDowell, G.R., Stickley, P.: Performance of geogrid-reinforced ballast. *Gr. Eng.* 39, 26–30 (2006)
  19. Desbrousses, R.L.E., Meguid, M.A., Bhat, S.: Effect of Temperature on the Mechanical Properties of Two Polymeric Geogrid Materials. *Geosynth. Int.* 1–31 (2021). <https://doi.org/10.1680/jgein.21.00032a>
  20. Desbrousses, R.L.E., Meguid, M.A.: Geogrids in cold climates: Insights from in-isolation tensile tests at low temperatures. In: *Geosynthetics: Leading the Way to a Resilient Planet.* pp. 467–473. CRC Press, London (2023)
  21. Desbrousses, R.L.E., Meguid, M.A.: On the Design of a Pneumatic Cyclic Loading Setup for Geotechnical Testing. In: *Society, C.G. (ed.) GeoSaskatoon 2023.* Canadian Geotechnical Society, Saskatoon, SK (2023)